Photodissociation and metastable decay of solvated cluster ions

Jack A. Syage
Aerophysics Laboratory, The Aerospace Corporation, Los Angeles, California 90009

(Received 19 June 1989; accepted 25 October 1989)

The stepwise solvation of dissociative ions was studied using a new technique in which a time-of-flight mass spectrometer is operated as a tunable low mass rejection filter. Two studies reflecting different modes of operation are reported. (1) Electronically excited aniline cation $C_6H_5NH_2^+$ was produced by picosecond photoionization and the rate of metastable dissociation to $C_5H_6^+ + HNC$ was investigated as a function stepwise solvation by NH_3. The addition of just one or two NH_3 solvent molecules was found to significantly reduce the rate of dissociation relative to the bare ion at comparable ion energies. (2) The resonant photodissociation of $(CH_3I)_n^+$ cluster ions, formed by electron impact (EI) ionization, was investigated in a crossed electron-laser-molecular beam configuration. No evidence for C–I dissociation, which is prominent in the bare ion, was observed. Instead van der Waals dissociation occurred by one- and two-photon mechanisms that varied depending on cluster size.

I. INTRODUCTION

An emerging field of molecular cluster work is concerned with understanding how the addition of solvent molecules, one at a time, modifies the behavior of chemical reactions.[1–4] Important topics include learning how unimolecular and bimolecular gas phase reactions are influenced by stepwise solvation or how large a solvent shell must be to make a bulk solution phase reaction energetically favorable in a small cluster.[4] Seeded clusters have great appeal because they represent an environment that is intermediate between the gas phase and the condensed phase.

In this work, we are interested in the photochemistry that occurs in cluster ions as a function of cluster size. The study of the size-specific photodissociation of clusters has progressed considerably in recent years as a result of tandem time-of-flight (TOF) mass filter arrangements that isolate specific cluster ion sizes for photodissociation, and mass resolve the resultant photofragments.[5–9] These advances have been applied more frequently to metal and semiconductor cluster ion studies[5–7] than to molecular cluster photochemistry.[8,9] Some of the first attempts to correlate molecular cluster ion dissociation to cluster size involved the study of metastable decay of neat cluster ions formed by multiphoton ionization and monitored by reflectron TOF devices.[10,11] Castleman and co-workers, for example, unraveled many details regarding $(NH_3)_n^+$ and $(CH_3OH)_n^+$ metastable dissociation.[10] However, reflectron studies of dissociation do not employ initial mass filtering and have a response time limit on the order of a microsecond.

We present a study of the effect of stepwise solvation on the dissociation of polyatomic ions. In one experiment $C_6H_5NH_2^+$, seeded in $(NH_3)_n$ solvent clusters, was excited using picosecond pulses to a metastable ion state. The relative rate of dissociation of the solvated versus unsolvated ion was then investigated. In another experiment, neat clusters of CH_3I were ionized by electron impact excitation and the cluster ions resonantly dissociated using nanosecond pulses. It was found that the dissociation of cluster ions is significantly modified relative to the monomer ion at comparable energies. Both sets of experiments made use of a new technique in which a standard three-grid TOF mass spectrometer is operated as a tunable low mass rejection filter.[12,13] This adaptation permits the elimination of successively larger cluster sizes from the photodissociation region, thus making possible the sensitive detection of size-specific cluster ion photodissociation against a zero background. Similar capabilities to date have been achieved only by tandem mass spectrometer arrangements.[5–9] The present method, on the other hand, is easily adapted to conventional single TOF mass spectrometers.

II. EXPERIMENT

The molecular beam TOF mass spectrometer is a conventional differentially pumped two chamber apparatus. Details of the vacuum system and data acquisition system have been described before.[4] Typical pulsed expansion conditions were 25 psi Ar, 500 μm nozzle diam, 400 μs pulse width, 2 cm nozzle–skimmer distance, and 1 mm diam skimmer. The ambient base pressure in the ionization chamber was typically 3×10^{-8} Torr, rising to about 2×10^{-7} Torr during operation of the pulsed nozzle at 10 Hz. The ion optics consist of the conventional three-grid configuration represented by V0, V1, and V2 in Fig. 1. Molecular beam (MB) ionization occurs in a field free volume by maintaining V1 = V2 during excitation. The additional elements V3 and V4 are part of a pulsed electron impact (EI) ionization source described in detail elsewhere.[14,15] For EI ionization, an electron beam (EB) pulse is admitted to the field-free excitation region by applying to V3 a 40 V gate pulse P3 (duration 200–400 ns). For MPI, a laser pulse is fired instead of P3.

The low mass rejection filter[13] operates by first applying a potential gradient (field) across the ionization region that

 0021-9606/90/031804-07$03.00

is negative with respect to the direction of the detector. This accelerates the ions away from the detector with the lighter masses exiting the lower V2 grid before the heavier masses. By reversing the field, the remaining higher masses are accelerated toward the detector to give a TOF mass spectrum that has the primary low masses filtered out. The pulse sequence for the TOF low mass filter (LMF) is shown in Fig. 1(b). Following ionization by EI or MPI, a voltage pulse P1 is applied to V1 to create the negative field. After P1, the field is reversed by applying P2 to V2. The dissociation of the remaining clusters by photodissociation (laser pulse L) or by metastable decay, *after* the P1 rejection pulse, produces fragment ions that appear on a zero background. A P1–P2 delay time may be introduced to lengthen the available time for metastable dissociation to occur. The cutoff mass for detecting larger cluster ions is tuned by adjusting the P1 pulse duration and/or voltage. The characteristics of the LMF can be accurately described by simple equations if we assume parallel plate flat fields.[13,16] We relate the position s(cm) and velocity v(cm/μs) of an ion as a function of the field E(V/cm), time t(μs), mass m(amu), and the charge $q(\pm 1)$ as follows:

$$s(t+t_i) = s(t_i) + v(t_i)t + \frac{0.482qEt^2}{m}, \quad (1)$$

$$v(t+t_i) = v(t_i) + \frac{0.965qEt}{m}, \quad (2)$$

where t_i is the initial time for t. The proportionality constants are specific to the units chosen above. The value of E in Eqs. (1) and (2) depends on when P1 and P2 are activated and which grid region the ions are located at any given time. The selectivity of the LMF near a nominal threshold mass m_0 is represented by the trajectory calculations in Fig. 2. The results for masses similar to m_0 that originate from the same initial position indicate that the cutoff condition is very sharp for relatively small ionization volumes. For ionization centered between the 1 cm V1–V2 grid spacing, one obtains the relation[13]

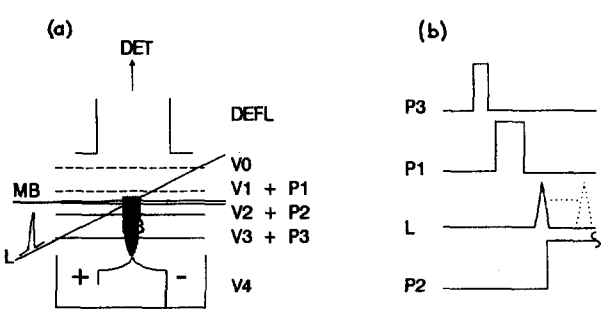

FIG. 1. (a) Configuration of the crossed electron-laser-molecular beam ion optics assembly. The direct current (dc) grid voltages are designated by V and the pulsed voltages by P. Deflector plates (DEFL) are used to compensate for ion drift resulting from the molecular beam (MB) velocity. Laser pulses are denoted by L and the detector by DET. (b) LMF pulse sequence. For EI excitation, P3 is activated. For MPI, a laser pulse is fired instead of P3.

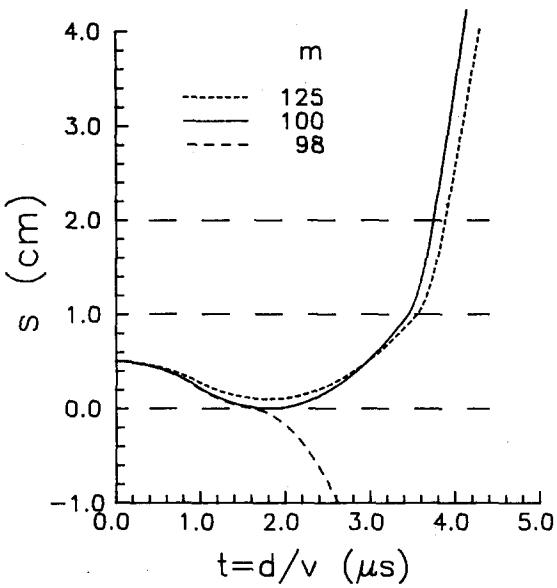

FIG. 2. Calculated ion trajectories s as a function of mass m. Grid positions are represented by the horizontal dashed lines. The position d of the ion along the molecular beam direction is a function of the molecular beam velocity v (5.6×10^4 cm/s for Ar). Calculations were based on; V1 = V2 = 1500 V, V3 = 1400 V, V0 = gnd, P1 = 60 V, P2 = 75 V, and $\tau_- = 1.0\,\mu$s.

$$m_0 = 0.965\,\frac{E_-(E_- - E_+)}{E_+}\,\tau_-^2, \quad (3)$$

where E_- is the negative field across the ionization region during the P1 rejection pulse period τ_-, and E_+ is the positive field that follows as a result of the P2 extraction pulse period. Equation (3) assumes successive P1 and P2 square pulses with no delay, and a P2 pulse duration that is longer than the time required for ions of mass $m > m_0$ to turn around. The use of a delay time between P1 and P2 for studying metastable ion decay alters the expression for m_0. For this case, we calculate actual trajectories to determine the expected cutoff mass value (cf. Sec. III A). The P1 pulse amplitude and duration was typically in the range of 20–80 V and 1–3 μs. The P2 extraction voltage was chosen to optimize space focusing, and the duration was maximized to extract the highest masses of interest. At present, our P2 pulse generator is limited to about 4 μs at 50–75 V, and hence the TOF mass resolution for larger cluster ions (e.g., $m > 300$ amu) deteriorated rapidly. A detailed description of the operational features and performance characteristics, including the effect of different ionization volume distributions on the instrument resolution, is presented in a separate paper.[13]

For studies where EI ionization preceded nanosecond laser photodissociation, it was necessary to externally trigger the laser Q-switch in order to synchronize the laser pulse with the P1, P2, and P3 pulse generators. For the $(CH_3I)_n^+$ photodissociation studies, nanosecond pulses were systematically varied in energy (up to 40 mJ) and entered the vacuum chamber either unfocused or defocused so that the beam diameter at the excitation region ($\sim$3 mm) closely matched the overlap of the molecular and electron beams. The picose-

cond laser is of the pulsed mode-locked design and does not have any convenient pretriggers with which to synchronize the firing of the EI ionizer and the laser pulse. We therefore used the picosecond laser only as a photoionization source and trigger for the LMF sequence. Pulses of about 0.1 mJ energy (at 266 nm) were focused to about 1 mm diam at the molecular beam. We are currently exploring methods for applying picosecond pump–probe excitation of ions following the LMF sequence outlined above.

III. RESULTS AND DISCUSSION

We begin by showing that the LMF can be used to remove successively larger seeded solvent shells M_n. This enables the chemical properties for specific size cluster ions to be studied. The REMPI ionization spectra in Fig. 3 were recorded by exciting clusters of aniline seeded in NH_3 at wavelengths longer than the aniline monomer $S_1(0,0)$ transition at 293.77 nm. The series of mass spectra in Fig. 3 compare the unfiltered spectrum to spectra employing successively greater levels of low mass filtering. This capability proved essential to the studies reported below.

A. Picosecond excitation and metastable decay of aniline$^+$–$(NH_3)_n$

In this section we present results pertaining to the stepwise solvation of the well known gas phase aniline cation metastable dissociation,[17–21]

$$C_6H_5NH_2^+ \rightarrow C_5H_6^+ + HNC.$$

The threshold energy for the bare ion dissociation, based on

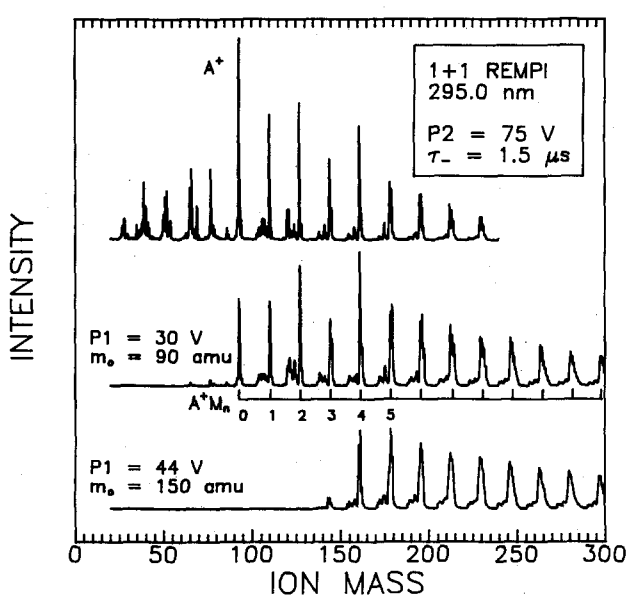

FIG. 3. A series of mass spectra showing successively higher levels of low mass filtering for aniline cation (A^+) solvated by an ammonia cluster shell (M_n). The top trace is unfiltered (i.e., P1 = 0). Ionization conditions were 1 + 1 REMPI using pulses of 295 nm, 5 ns, 1.0 mJ. The deflector voltages were adjusted to enhance the detection of larger cluster.

$C_5H_6^+$ appearance energy measurements, has been reported to be 11.3 eV above the neutral ground state,[20] however on a microsecond time scale no product is observed at energies as high as 13 eV.[20,21] The measured dissociation rate at 14.0 eV photon energy (two-photon ionization, one-photon ion absorption using 266 nm pulses) is $k \sim 1$–$2\ \mu s^{-1}$,[18,19] although the ion energy in these experiments was uncertain because the energy of the ionized electron was not known. Measurements by PIPECO, which establish the ion energies, yielded a similar rate at an ion energy of 13.5–13.6 eV.[17] This would correspond to excitation into the tentatively assigned $\tilde{E}$ electronic state of the aniline cation.[17]

In recent work, we investigated the chemistry of the aniline cation seeded in various hydrogen bonding molecular clusters in order to gain a better understanding of the influence of stepwise solvation on reactive ions.[4] The relative rates of the solvated dissociation were evaluated by examining fragment ion signals in the mass spectrum that reflected the competition between the above metastable dissociation and the absorption of a fourth photon leading to other fragmentation channels. The results for the three-photon ionization/excitation of aniline–$(N_2H_4)_n$ indicated that $k > \tau_L^{-1}$ at 232 nm and $k < \tau_L^{-1}$ at 266 nm where τ_L was the laser pulse duration of about 5 ns. The proton affinic solvent molecules were found to bind to the amine group of aniline.[4] Consequently, dissociation caused the solvent to depart with the neutral product HNC, which made it difficult to distinguish $C_5H_6^+$ fragments that originated from bare vs solvated aniline cation. The case for N_2H_4 solvation proved fortuitous because the low ionization potential of N_2H_4 (8.74 eV) led to an unusual electron transfer from the solvent to $C_5H_6^+$ *during* dissociation to give HNC–$(N_2H_4)_n^+$. This made possible the detection of solvated dissociation.[4] In general one would like to be able to assign an unsolvated fragment ion (e.g., $C_5H_6^+$) to a specific solvated parent ion. In this work, we rely on the LMF technique[13] to make this distinction and compare relative rates of metastable dissociation for unsolvated versus solvated aniline cation by monitoring the $C_5H_6^+$ ion. We report our findings for the aniline$^+$–$(NH_3)_n$ cation system (henceforth A^+M_n).

The LMF sequence enables fragmentation that occurs after the P1 pulse (either by photodissociation or metastable decay) to appear in the TOF mass spectrum. To increase the time available for observing metastable decay, a field-free reaction period was introduced in the form of a delay time τ_{del} between P1 and P2. The size of the solvent cluster bound to A^+, from which a detected $C_5H_6^+$ fragment originates, can be tuned by adjusting the P1 voltage to remove successively larger parent cluster sizes from the reaction period. The principle is illustrated by the calculated trajectories in Fig. 4 for aniline cation (A^+, 93 amu) and the metastable decay product $C_5H_6^+$ (a^+, 66 amu), as a function of the level of solvation M_n. We consider three mechanisms for the production of a^+ fragment: prompt dissociative ionization (denoted by a_1^+), metastable decay from unsolvated A^+ (a_2^+), and metastable decay from solvated A^+ (a_3^+). In Fig. 4(a) metastable decay that occurs during the field-free τ_{del} period gives rise to fragment a_2^+ that is detected despite LMF conditions that otherwise reject primary ions below

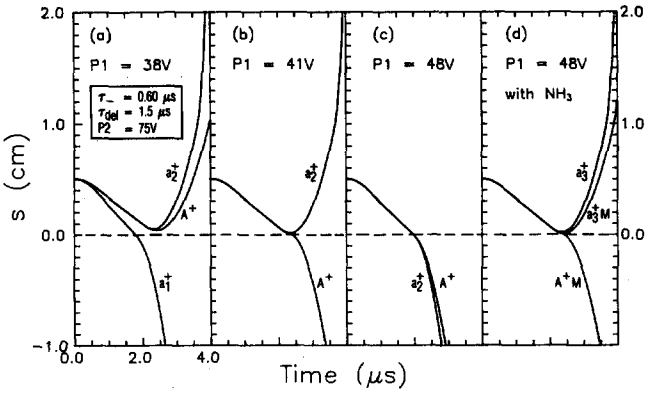

FIG. 4. Calculated trajectories for metastable decay of aniline cation (A^+, 93 amu) to fragment $C_5H_6^+$ (a^+, 66 amu). (a)–(c) unsolvated A^+ under increasing LMF conditions. (d) Solvated A^+ with NH_3 (M, 17 amu) under the LMF conditions of (c). Fragment a^+ can be produced by prompt dissociation (a_1^+), metastable decay of unsolvated A^+ (a_2^+), and metastable decay of solvated A^+M (a_3^+). Grid spacings and voltages are the same as in Fig. 2 unless otherwise stated. The position of the lower "reflecting" grid is indicated by the dotted line.

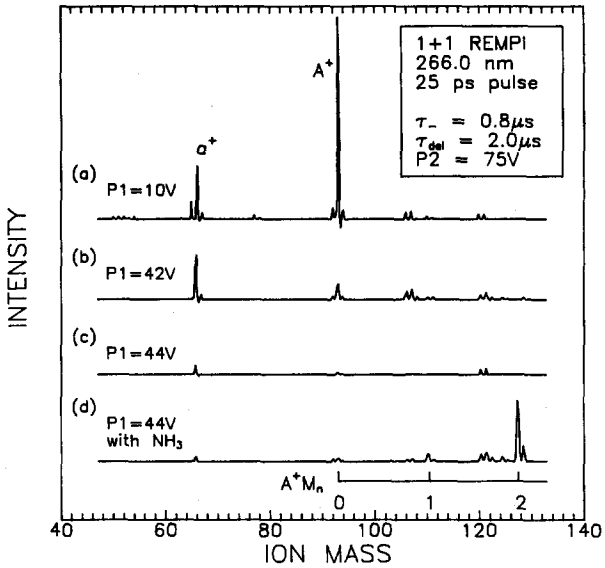

FIG. 5. Metastable decay of unsolvated and solvated aniline cation (A^+) formed by 1 + 1 REMPI using 266 nm, 25 ps, 0.1 mJ pulses. (a)–(c) The LMF conditions were increased to reject A^+ while detecting the metastable decay fragment a^+. (d) Introduction of NH_3 to form solvated aniline cation A^+M_n under the LMF conditions of (c). Spectra (a)–(d) correspond closely to the predicted behavior in Figs. 4(a)–(d).

mass 85 amu (e.g., a_1^+). This occurs because the LMF operates as an energy filter in the τ_{del} mode (in much the same way as a reflectron). If dissociation occurs during the field-free interval, then the kinetic energy of a_2^+ is less than that for A^+ ($\Delta E = \Delta m v^2/2$). As a result, the subsequent P2 extraction pulse is more effective at reflecting a_2^+ than A^+. In Fig. 4(b) it is shown that, by increasing the P1 voltage, it is possible to reject A^+ and still detect the metastable product a_2^+. The presence of ion masses substantially below the threshold value m_0 is therefore compelling evidence for metastable decay processes. The solvation of A^+ metastable decay can be investigated by further increasing the P1 voltage until a_2^+ from the monomer dissociation is rejected [Fig. 4(c)]. The presence of a_3^+ in the LMF mass spectrum can then be attributed to AM_n^+ metastable dissociation [Fig. 4(d)].

Picosecond pulses (two-photon ionization, one-photon excitation at 266 nm) were used because the high peak powers ($\sim$500 MW/cm^2) create transition rates that effectively compete with fast intermediate decay processes (e.g., van der Waals dissociation), whereas the low total energies ($\sim$0.1 mJ/pulse, 25 ps) minimize the probability that a fourth photon is absorbed leading to fragmentation. Under our conditions, we estimate a relative proportion of four-photon vs three-photon excitation of <0.10.[22] This estimate is consistent with the observed mass spectrum in Fig. 5(a), which is remarkably free of fragmentation other than for the metastable reaction product $C_5H_6^+$. The series of REMPI mass spectra in Fig. 5 demonstrate the model described above. The spectrum, for a weak P1 rejection pulse, consists of a distribution of primary fragment ions including a_1^+ [Fig. 5(a)]. An increase in P1 removes all fragment ions except for a_2^+. In Fig. 5(b), it is shown that one can eliminate A^+ and still observe the presence of the metastable product a_2^+, as predicted in Fig. 4(b). Further increase of P1 eventually removes the a_2^+ signal that derives from A^+ [Fig. 5(c)], again in agreement with calculations [Fig. 4(c)]. NH_3 was then introduced under the same LMF conditions to probe for metastable decay from solvated A^+. In Fig. 5(d), A^+ and A^+M are eliminated, but the higher solvated species are detected, in accord with Fig. 4(d). The virtual absence of a^+ under these conditions, however, indicates that the metastable dissociation from solvated species A^+M_n is effectively quenched over the time scale of τ_{del}. In principle, one can vary τ_{del} to derive rate constants for the dissociation. We place an upper limit of $k < 0.2\,\mu s^{-1}$ for the solvated metastable dissociation, which is about an order of magnitude slower than the unsolvated rate.[18,19] It is not certain whether the dissociation rate is actually reduced or perhaps quenched by the removal of energy due to solvent evaporation. However, our earlier study showing extensive dissociation in N_2H_4 microsolvents argues for the former conclusions.

B. Photodissociation of $(CH_3I)_n^+$ cluster ions

The photodissociation of solvated CH_3I^+ ion was chosen because the spectroscopic[12,23,24] and dissociative[25–29] properties of the monomer ion are reasonably well known. Low energy EI ionization of $(CH_3I)_n$ clusters produces a distribution of electronically excited cluster ions, of which only those formed in the ground $\tilde{X}$ state survive van der Waals (vdW) dissociation.[30] We investigated the $\tilde{A} \leftarrow \tilde{X}(^2\Pi_{1/2})$ (upper ground spin–orbit state) resonant transitions in the $(CH_3I)_n^+$ clusters at wavelengths of 580–600 nm. The $\tilde{A} \leftarrow \tilde{X}(^2\Pi_{1/2})$ spectrum of CH_3I^+ monomer

exhibits a highly structured and extensive Franck–Condon progression in the ν_3 C–I stretch mode. A predissociation threshold to $CH_3^+ + I$ occurs at a wavelength of 596 nm due to internal conversion to the dissociative limit of the $\tilde{X}$ state.[23] This corresponds to an energy of about 2500 cm^{-1} above the $\tilde{A}$ origin. The lifetime of the $\tilde{A}$ state internal conversion and the subsequent $\tilde{X}$ dissociation near threshold have been estimated to be about 4[31] and 100 ns,[23] respectively.

The means for studying photodissociation from specific cluster ion sizes $(CH_3I)_n^+$ is illustrated in Fig. 6. Mass spectra are presented that represent the sequence of events: ionization, low mass rejection, and photodissociation. The 30 eV EI ionization mass spectrum is shown in Fig. 6(a). The LMF P1 pulse was adjusted to remove all masses below the dimer ion [Fig. 6(b)]. Subsequent photodissociation by the resonant 595 nm excitation gives rise to the vdW dissociation $CH_3I^+ + CH_3I$ as seen in Fig. 6(c). Differentiating the photofragment parent from among the remaining higher mass clusters is accomplished by filtering out successively larger cluster sizes and observing the disappearance of the corresponding photofragments. The difference spectrum from successive mass spectra consists of a single cluster ion parent and associated fragments as shown in Fig. 7 for the dimer cation dissociation. A spectrum consisting of *only* the dimer species is obtained by subtracting, from Fig. 6(b), the LMF mass spectrum corresponding to removal of all masses below the trimer ($m_0 = 350$ amu). By this method, a window of ion masses $200 < m < 350$ amu is selected as viewed in Fig. 7(a). (The mass window can be made narrower for more demanding mass discrimination needs.[13]) The corresponding difference spectrum in the presence of the 595 nm resonance dissociation pulse reveals, in Fig. 7(b), the photoproduct for dimer cation dissociation. Finally, subtracting Fig. 7(a) from Fig. 7(b) gives a spectrum [Fig. 7(c)] consisting of the photoproduct as a positive signal and the parent ion as a negative signal. Figure 7(c) clearly shows that the absorbing species is $(CH_3I)_2^+$ and not $(CH_3I)I^+$ (at mass 269). In practice, the subtraction of entire spectra is not actually necessary; the same information on size-specific dissociation can be obtained by simply subtracting the measured intensities from the appropriate pairs of LMF mass spectra. This procedure was used in the present work for the larger cluster ions.

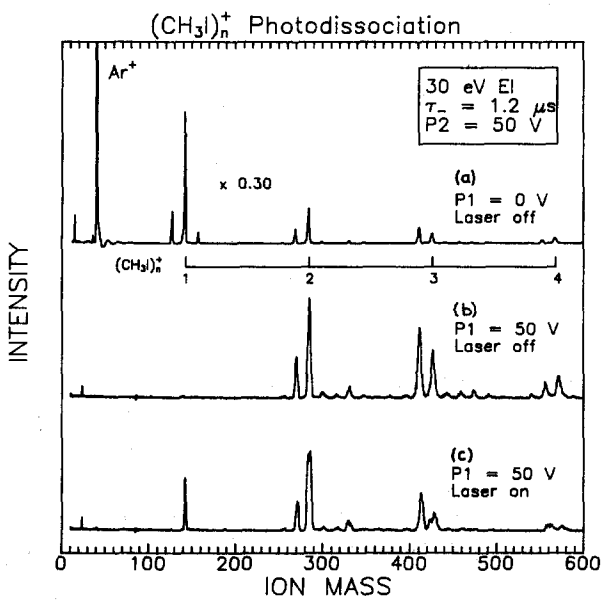

FIG. 6. Mass specific resonance photodissociation of $(CH_3I)_n^+$. (a) 30 eV EI mass spectrum (Ar^+ peak has been clipped and is ~3× larger than shown); (b) LMF rejection of monomer CH_3I^+; (c) same as above, but with resonance excitation at 595.2 nm.

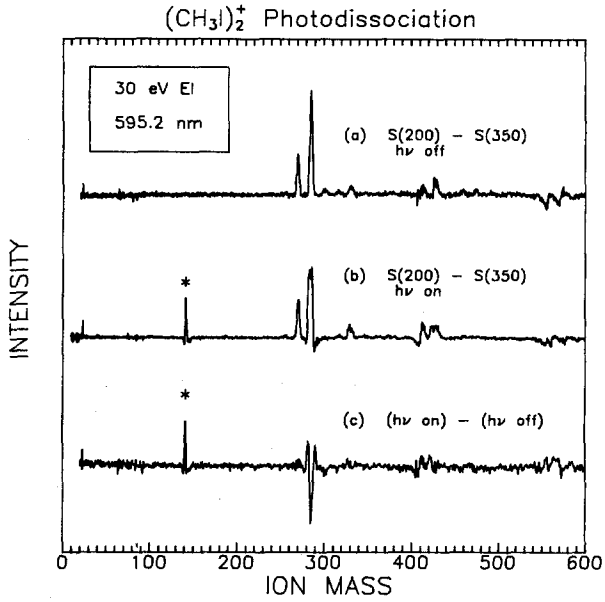

FIG. 7. Mass specific resonance photodissociation of $(CH_3I)_2^+$. (a) Window spectrum for dimer only, obtained from the difference of the LMF spectra $S(m_0)$ for $m_0 = 200$ and $m_0 = 350$ amu. (b) Corresponding difference spectrum showing dimer photodissociation to CH_3I^+ (*) (595.2 nm, 35 mJ, unfocused). (c) Parent (negative signal) and fragment (positive signal) spectrum obtained by subtracting spectrum (a) from (b). Conditions were 30 eV EI ionization, 5% CH_3I in 25 psi Ar.

The only significant dissociation channel observed for $(CH_3I)_2^+$ was the vdW dissociation to give $CH_3I^+ + CH_3I$, by a single-photon process. The LMF spectra for successively larger cluster ion sizes revealed that the monomer photoproduct CH_3I^+ is produced by one-photon absorption in the trimer, but only by two-photon absorption in the tetramer and pentamer. These determinations were made by measuring the laser power dependence for all photoproducts. Interestingly, the prominent monomer cation dissociation $CH_3I^+ \rightarrow CH_3^+ + I$ was *not* observed for any size cluster, despite undergoing excitation to energies that exceeded the threshold for this reaction. The observed cluster ion van der Waals photodissociation pathways are summarized in the following:

$$(CH_3I)_n^+ \rightarrow (CH_3I)_{n-m}^+ + m(CH_3I)$$

$n = 2$: $m = 1$ (one-photon) ...

$n = 3$: $m = 1,2$ (one-photon) ...

$n = 4$: $m = 1,2$ (one-photon) $m = 3$ (two-photon)
$n = 5$: $m = 1,2,3$ (one-photon) $m = 4$ (two-photon).

The wavelength-resolved photodissociation spectrum of $(CH_3I)_2^+$ was recorded by monitoring the photoproduct signals CH_3I^+ and CH_3^+. Dimer cations were selected by LMF rejection of the initially ionized monomer ions and by adjusting the expansion conditions to minimize clusters larger than dimer. The recorded spectrum was structureless over the range studied (580–600 nm). Production of CH_3I^+ extended well below the low energy limit for one-photon dissociation of monomer CH_3I^+ to $CH_3^+ + I$. At these longer wavelengths the vdW dissociation is the only energetically feasible dissociation. Excitation at shorter wavelengths, however, failed to reveal the energetically allowed C–I bond dissociation that is prominent in the monomer cation. Apparently, the weaker vdW bond dissociates preferentially and leaves insufficient internal energy in the monomer fragment ion CH_3I^+ to dissociate the C-I bond. An attempt was made to photodissociate the CH_3I^+ fragment by exciting $(CH_3I)_2^+$ at wavelengths that also resonantly dissociate CH_3I^+. Again, no significant appearance of CH_3^+ was observed, suggesting that the dimer photodissociation lifetime may be greater than the laser pulse duration of 5 ns, or that the CH_3I^+ photoproduct is formed in vibrational levels that have poor Franck–Condon factors for excitation.

If the lifetime of the van der Waals bond is indeed greater than 5 ns and, therefore, not significantly less than the reported lifetime of about 100 ns[23] for C–I bond cleavage at 595 nm, then one might expect to see evidence of C–I bond breaking in the cluster ion photodissociations. The absence of this channel is consistent with a cluster ion predissociation mechanism in which the rate limiting step is radiationless decay from $\tilde{A}$ to vibrationally excited levels of the ground electronic state, followed by a vdW dissociation that is faster than C–I bond dissociation. A test of this mechanism awaits experiments that can independently excite the cluster ion and the CH_3I^+ photoproduct with suitably long delay times. Such experiments will also make it possible to determine whether the two-photon pathway to photoproducts in the larger clusters ($n > 3$) is concerted (i.e., two-photon reactant excitation) or sequential (one-photon reactant, one-photon product excitation).

IV. SUMMARY AND CONCLUSIONS

One of the fundamental issues in chemical dynamics is understanding how solvent molecules influence the properties of chemical reactions. This has traditionally been investigated by comparing the kinetics of gas phase reactions to that in solvents of varying viscosity. Our approach in this paper is to examine how a gas phase reaction is modified by the stepwise addition of single solvent molecules. In one study, electronically excited aniline cation $C_6H_5NH_2^+$ was produced by picosecond photoionization and the rate of metastable dissociation to $C_5H_6 + HNC$ was investigated for the bare parent ion and in solvent clusters of NH_3. The gas phase rate of dissociation was reduced by an order of magnitude or more to $k < 0.2\,\mu s^{-1}$ by the addition of just one or two NH_3 molecules. In a second study, $(CH_3I)_n^+$ clusters, formed by EI ionization, were mass filtered to select specific cluster sizes, which were then resonantly photodissociated. Although excitation to the monomer cation $\tilde{A}$ state dissociates to form $CH_3^+ + I$, similar excitation of the clusters exhibited only van der Waals dissociation. Distinct one- and two-photon product pathways were unraveled for cluster sizes up to $n = 5$.

The study of dissociation from *specific* cluster sizes was made possible by employing a new technique in which a standard TOF mass spectrometer is operated as a tunable low mass rejection filter. The device permits ion photoproducts to be observed against a zero background for sensitive detection, and can be tuned to reject successively larger cluster sizes prior to dissociation. The LMF consists of a single TOF assembly and will therefore not match the mass selectivity of more elaborate tandem mass spectrometer systems. However, it is easily adpatable to standard TOF mass spectrometers and, hence, is a sensible choice for many ion and cluster ion photodissociation studies.

ACKNOWLEDGMENTS

I am grateful for the experimental and software assistance provided, respectively, by Jhobe Steadman and Eric Fournier. This work was supported by the Aerospace Sponsored Research program.

[1] O. Cheshnovsky and S. Leutwyler, J. Chem. Phys. **88**, 4127 (1988); O. Cheshnovsky and S. Leutwyler, Chem. Phys. Lett. **121**, 1 (1985).
[2] D. Solgadi, C. Jouvet, and A. Tramer, J. Phys. Chem. **92**, 3313 (1988); B. Brutschy, C. Janes and J. Eggert, Ber. Bunsenges, Phys. Chem. **92**, 74 (1988).
[3] J. F. Garvey and R. B. Bernstein, Chem. Phys. Lett. **143**, 13 (1988); J. F. Garvey and R. B. Bernstein, J. Am. Chem. Soc. **109**, 1921 (1987); J. F. Garvey and R. B. Bernstein, J. Phys. Chem. **90**, 3577 (1986).
[4] J. A. Syage, J. Phys. Chem. **93**, 170 (1989); J. A. Syage and J. Steadman, Chem. Phys. Lett. (in press).
[5] L. A. Bloomfield, R. R. Freeman, and W. L. Brown, Phys. Rev. Lett. **54**, 2246 (1985).
[6] Q.-L Zhang, Y. Liu, R. F. Curl, F. K. Tittle, and R. E. Smalley, J. Chem. Phys. **88**, 1670 (1988).
[7] S. M. Beck and J. Andrews, J. Chem. Phys. **91**, 4420 (1989); K. LaiHing, P. Y. Chen, T. G. Taylor, K. F. Willey, M. Peschke, and M. A. Duncan, Anal. Chem. **61**, 1458 (1989).
[8] M. Okumura, L. I. Yeh, and Y. T. Lee, J. Chem. Phys. **83**, 3705 (1985); M. Okumura, L. I. Yeh, J. D. Meyers, and Y. T. Lee, *ibid.* **85**, 2328 (1986).
[9] D. E. Hunton, M. Hofmann, T. G. Lindeman, C. R. Albertoni, and A. W. Castleman, Jr., J. Chem. Phys. **82**, 2884 (1985).
[10] O. Echt, P. D. Dao, S. Morgan, and A. W. Castleman, Jr., J. Chem. Phys. **82**, 4076 (1985); R. G. Keesee and A. W. Castleman, Jr., in *Ion and Cluster Ion Spectroscopy and Structure*, edited by J. P. Maier (Elsevier, New York 1989).
[11] U. Boesl, H. J. Neusser, R. Weinkauf, and E. W. Schlag, J. Chem. Phys. **86**, 4857 (1982).
[12] J. A. Syage, J. E. Pollard, and J. Steadman, Chem. Phys. Lett. **161**, 103 (1989).
[13] J. A. Syage and J. Steadman, Rev. Sci. Instrum. (in press).
[14] J. A. Syage, Chem. Phys. Lett. **143**, 19 (1988).
[15] J. E. Pollard and R. B. Cohen, Rev. Sci. Instrum. **58**, 32 (1987).
[16] W. C. Wiley and I. H. McLaren, Rev. Sci. Instrum. **26**, 1150 (1955).
[17] T. Baer and T. E. Carney, J. Chem. Phys. **76**, 1304 (1982).
[18] D. Proch, D. M. Rider, and R. N. Zare, Chem. Phys. Lett. **81**, 430 (1981).
[19] H. J. Neusser, H. Kühlewind, U. Boesl, and E. W. Schlag, Ber. Bunsenges. Phys. Chem. **89**, 276 (1985); H. Kühlewind, H. J. Neusser, and E. W. Schlag, J. Chem. Phys. **82**, 5452 (1985).
[20] C. Lifshitz, P. Gotchiguian, and R. Roller, Chem. Phys. Lett. **95**, 106 (1983).

[21]M. L. Gross, Org. Mass Spectrom. **6**, 827 (1972): P. Brown, Org. Mass Spectrom. **3**, 639 (1970).
[22]A laser pulse of $\tau = 20$ ps duration, 0.1 mJ, and 266 nm, focused to 1 mm diam at the molecular beam corresponds to a power density of 500 MW/cm^2 and a photon flux I of 6.6×10^{26} photons s^{-1} cm^{-2}. Using the reported cross section of $\sigma = 5\times10^{-18}$ cm^2 for the absorption of a fourth photon (Ref. 17) leads to a probability for that event of $\sigma I\tau = 0.066$.
[23]K. Walter, R. Weinkauf, U. Boesl, and E. W. Schlag, J. Chem. Phys. **89**, 1914 (1988); R. Weinkauf, K. Walter, U. Boesl, and E. W. Schlag, Chem. Phys. Lett. **141**, 267 (1987).
[24]A. M. Woodward, S. D. Colson, W. A. Chupka, and M. G. White, J. Phys. Chem. **90**, 274 (1986); W. A. Chupka, S. D. Colson, M. S. Seaver, and A. M. Woodward, Chem. Phys. Lett. **95**, 171 (1983).
[25]J. H. D. Eland, R. Frey, A. Kuestler, H. Schulte, and B. Brehm, Int. J. Mass Spectrom. Ion Phys. **22**, 155 (1976).
[26]D. M. Mintz and T. Baer, J. Chem. Phys. **65**, 2407 (1976).
[27]S. P. Goss, D. C. McGilvery, J. D. Morrison, and D. L. Smith, J. Chem. Phys. **75**, 1820 (1981).
[28]D. M. Szaflarski and M. A. El-Sayed, J. Phys. Chem. **92**, 2234 (1988).
[29]M. Kawasaki, H. Sato, T. Kikuchi, S. Kobayashi, and T. Arikawa, J. Chem. Phys. **87**, 5739 (1987); M. Tadjeddine, G. Bouchoux, L. Malegat, J. Durup, C. Pernot, and J. Weiner, Chem. Phys. **69**, 229 (1982).
[30]J. A. Syage and J. Steadman (to be submitted).
[31]P. C. Cosby and J. T. Moseley, unpublished results; see Ref. 29(b).